Inducing the Rotation of a Single Phenyl Ring with Tunneling Electrons

N. Henningsen,[†] K. J. Franke,[†] I. F. Torrente,[†] G. Schulze,[†] B. Priewisch,[‡] K. Rück-Braun,[‡] J. Dokić,[§] T. Klamroth,[§] P. Saalfrank,[§] and J. I. Pascual*[,†]

Institut für Experimentalphysik, Freie Universität Berlin, Arnimallee 14, 14195 Berlin, Germany, Institut für Chemie, Technische Universität Berlin, Strasse des 17. Juni 135, 10623 Berlin, Germany, and Institut für Chemie, Universität Potsdam, Karl-Liebknecht-Strasse 24-25, 14476 Potsdam-Golm, Germany

Received: May 30, 2007; In Final Form: July 19, 2007

We report on the electron induced intramolecular rotation of a single phenyl ring of an azobenzene derivative adsorbed on a Au(111) surface using a low-temperature scanning tunneling microscope (STM). By proper functionalization of each of the two azobenzene's phenyl rings with CN end groups, we are able to identify two distinct isomers at the metal surface corresponding to two possible alignments of the functional groups in the trans conformer. Tunneling electrons induce molecular motion and intramolecular conformational changes both on isolated molecules and H-bonded molecular islands. Particular enhancement is observed for the electrons resonantly tunneling through affinity levels, which is consistent with electronic molecular excitations as the basic mechanism for this manipulation process. On the basis of quantum chemical calculations of a free azobenzene molecule, we propose a dynamical model for the ring-rotation pathways, which includes the electric field in the STM junction to effectively couple electronic excitation with intramolecular rotations.

Understanding the conformational dynamics of molecular functional units upon excitation is important for developing effective control strategies of their properties through external stimuli.[1] Recently, the interest of molecular photoswitches in condensed matter has grown following the rapid development of precise molecular epitaxy tools for the "bottom up" growth of molecular devices with possible applications to information processing, storage, or switching. Among all the processes which can lead to the control of molecular function with light, the cis−trans photoisomerization is one of the best understood in solution or in gas phase.[2] Photoisomerization of azobenzene involves single states, which are populated upon irradiation with ∼320 and ∼420 nm light, allowing effective control of its structure by external stimuli.[3−7]

The dynamics of molecular switches adsorbed on metal surfaces is expected to be different than in the gas phase because of the existence of effective surface-mediated mechanisms for the rapid quenching of molecular excitations,[8] to the rigidity of the bonding to the substrate, and to the ubiquitous interactions between molecules in the condensed phase. In spite of these, recent scanning tunneling microscopy (STM) experiments have shown that the conformation of molecular switches can be modified through the inelastic excitation of vibrations[9−12] or by the effect of the electric field.[13−15] Electronic excitations can also have an important role. For atoms and molecules on semiconductor surfaces, they are primarily involved in dissociative or switching dynamics.[16−18] This paper reports about the manipulation of the internal conformation of single azobenzene molecules on a metal surface through electronic excitations using a low-temperature scanning tunneling microscope.

Our studies are done on 3,3′-dicyanoazobenzene (di-meta-cyanoazobenzene: DMC) adsorbed on a Au(111) surface. Here, the phenyl rings of the azobenzene molecule have been functionalized with two cyano (CN) groups located at meta sites.[19,20] This functional group is widely used as a marker in optical spectroscopy. In our study, the functionalization of meta sites helps to identify the rotation of one phenyl ring around its connection to the azobenzene backbone (NC bond). This rotation is indicated by the angle β in Figure 1a. The cyano substituents are highly electrophilic,[21] which may favor the stabilization of the planar adsorption configuration on the Au(111) surface. On the other hand, the general properties of azobenzene (structure and electronic configuration)[22,23] are not expected to be strongly modified upon adsorption.

Quantum chemical calculations of potential energy surfaces (PES) for both the neutral DMC specie and the negative ion found that in both cases cis and trans isomers can be connected through one single PES.[24] Conformational dynamics along neutral isomerization pathways have also been experimentally demonstrated for DMC in solution.[19]

When adsorbed on a surface, another molecular conformation may also be important. The β rotation of a phenyl ring is usually ignored in gas phase or solution experiments because the rotation barrier is small. At the surface, this rotation is further frustrated by the affinity of the aromatic groups to adsorb planar to a metal surface, thus, leading to only two possible β orientations (Figure 1). Recent experiments on a different molecular specie found that intramolecular rotation of phenyl end groups can occur erratically after thermal excitation.[25] Here, we report on the controlled rotation of a single phenyl ring of *trans*-DMC between two possible orientations induced by tunneling electrons. With the help of tunneling spectroscopy measurements, we propose a mechanism in which the manipulation is activated by the transient population of negative ion states. To model the intramolecular dynamics, we have performed quantum chemistry calculations of a free DMC molecule, which reveal that the ring rotation probably follows along a neutral pathway after the short-lived excitation. An interesting result of our model is that the

* Corresponding author.
[†] Freie Universität Berlin.
[‡] Technische Universität Berlin.
[§] Universität Potsdam.

10.1021/jp0741861 CCC: $37.00
Published on Web 09/19/2007

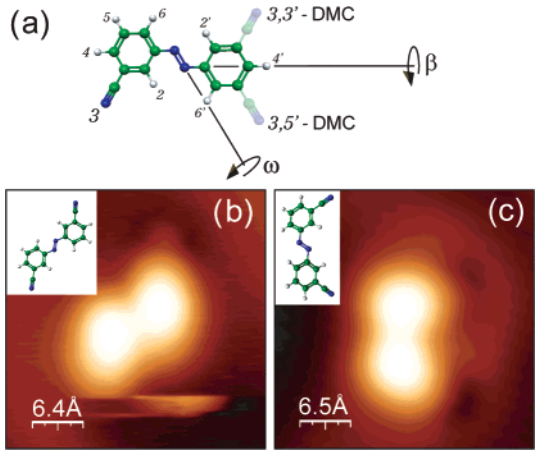

Figure 1. (a) Atomic model of the DMC molecule indicating the rotational axis around which the dihedral angle β is defined (leading to the rotation of a phenyl ring from 3,3′ to the 3,5′ conformation) and the axis of ω-angle rotation (leading to the cis−trans isomerization). STM images of (b) the DMC 3,3′ and (c) 3,5′ isolated isomers on the Au(111) surface (3.2 × 3.2 nm^2; $I_t = 0.48$ nA; (b) $V_s = -1$ V; (c) $V_s = +1.16$ V).

coupling of electronic excitations with intramolecular rotations is only effective if the relaxed molecular structure at the surface is nonplanar. Thus, the role of the interaction with the metal surface or, as modeled here, the electric field in the STM junction is crucial to understand the switching dynamics.

I. Experimental Section

The experiments were carried out in a custom-made low temperature (5 K) scanning tunneling microscope under ultra-high vacuum conditions. A Au(111) single crystal was chosen as a substrate, since molecular adsorption on this surface is generally weak. The surface was cleaned by repetitive cycles of 1 keV Ne^+ ion sputtering and annealing to 750 K, resulting in an atomically clean surface with the 22 × $\sqrt{3}$ reconstruction.[26] DMC molecules were sublimated from a custom-made Knudsen cell ($T_{sub} \sim 370$ K) onto the Au(111) surface. To limit transient motion of molecules at the surface and to avoid the formation of ordered molecular domains, the substrate temperature was kept below 100 K during dosing. All STM measurements were performed at 5 K.

II. Results and Discussion

A. DMC Conformation on Au(111). When a submonolayer amount of DMC is deposited on Au(111) at low-temperature, we find mostly disordered islands with a few number of monomers. There are two characteristic configurations of the molecules as shown in Figure 1b,c. Both can be described by two ellipsoidal lobes separated by 0.74 ± 0.05 nm, one from the other. Each lobe corresponds to one of the phenyl moieties. The cyano groups induce a weak elliptical deformation of the lobes in the STM topographs. In isolated molecules on the gold surface, it is also possible to observe faint topographic depressions close to the location of the end groups (Figure 1b,c). Since the cyano substituent is highly electron attracting,[21] we can speculate that these depressions are due to a local increase of the work function around the negatively charged part of the molecule.

The difference between the two characteristic shapes of the molecules is the relative orientation of the ellipsoidal lobes. They can be described as having either an inversion center at their central N═N double bond (Figure 1b) or a mirror plane (Figure 1c) in their middle. These two are the only equilibrium structures found on the Au(111) surface, and we relate them to two different conformations of the DMC molecule. The features in Figure 1b correspond to the trans isomer exposing the two CN terminations in opposite directions. The mirror symmetry of features like in Figure 1c might resemble the shape of a cis isomer forced to have a planar conformation due to the interaction with the surface.[10] However, these species correspond instead to another version of the trans isomer, characterized by a β rotation of 180° with respect to the one described above, that is, with a CN group in *5′-meta* instead in *3′-meta* site.[27] Since the azo backbone (C—N═N—C) is not affected by this transformation, we distinguish them here as 3,3′- and 3,5′-DMC. Both conformers are electronically identical and are expected to be stabilized with similar probability upon adsorption. Although structurally inequivalent, our STM cannot resolve clear differences between the 3,5′ and 5,3′ trans isomers, nor between 3,3′ and 5,5′ isomers; consequently, we treat them here as equivalent.

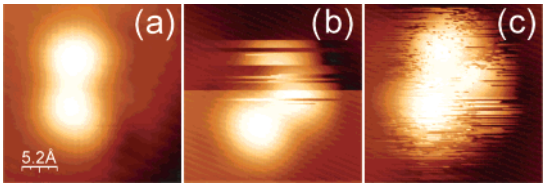

Figure 2. (a) STM images of an isolated molecule scanned with several sample bias values. (a) For $V_s = 1.2$ V the molecule lies stable on the Au(111) surface with a 3,5′ conformation. (b) For $V_s = 1.5$ V molecular motion between two configurations is excited. (c) For $V_s = 1.8$ V the molecule moves faster than the scanning process, appearing with a diffuse shape (images, 2.6 × 2.6 nm^2, $I_t = 0.21$ nA).

B. DMC Conformational Changes. Molecular motion (diffusion and rotation) was frequently induced by the STM tip during scanning. In general, imaging of islands and monomers becomes unstable when the sample bias was raised above a threshold value of about 1.5 eV. Figure 2 shows a series of STM images of an isolated molecule showing that the successive increase of the voltage (V_s) is accompanied by an instability of the molecule on the Au(111) surface. In Figure 2a, the DMC molecule lies stable with a 3,5′ conformation while scanned with $V_s = 1.2$ V. When the sample bias is increased to $V_s = 1.5$ V, horizontal lines in the image indicate erratic changes of the molecule during scanning. As the bias is increased to $V_s = 1.8$ V, the switching rate becomes faster (~7 Hz), and the STM only has the ability of imaging a superposition of two positions.

In some occasions, the induced motion of the whole molecule is accompanied by a change in molecular conformation between the 3,3′ and the 3,5′ isomers. Figure 3a,b shows one example where a 3,5′ conformer appears as 3,3′ after applying a current pulse of 10 nA for 4 s ($V_s = 1.8$ V). Since both internal and external changes are induced simultaneously, we tentatively ascribe this phenomenon to the existence of a transient state with high mobility, which is excited by tunneling electrons. Surprisingly, in rare occasions, a double ring-flip could be detected after a single pulse event, leading to an apparent change in the chiral aspect of the molecule in the STM image (Figure 3c,d). STM cannot resolve the structure of the DMC neck bone, and therefore, we cannot exclude in this case a flipping mechanism in which the molecule is reversed as a whole.

Similar electron-induced motion can also be observed during scanning with similar high bias values or by applying voltage pulses on bi-dimensional (disordered[29]) molecular islands. DMC molecules coalesce easily in islands interconnected very prob-

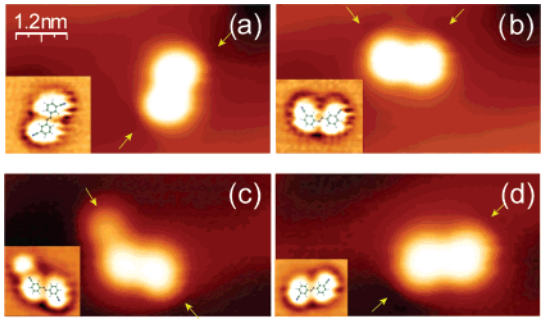

Figure 3. STM images of isolated DMC molecules before and after applying current pulses with the tip of the STM on top of one of the phenyl rings. (b) shows the same molecule as in (a) resulting after applying a 4 s bias pulse of 1.8 V with a current of 10 nA. A combination of translation, rotation, and a change from 3,3′ to 3,5′ conformation can be seen. To guide the reader's eye, arrows point to the faint depressions around the location of the CN end groups. Additionally, the inset in each figure shows the STM topographs treated with a Laplace filter[28] (to emphasize the molecular shape) and an atomistic model of the molecular conformation. In (c) and (d), the same procedure (now a 0.5 s. pulse) leads to a double change from 3,3′ to 5,5′ conformation (a complete inversion to its chiral form in two dimensions can also not be excluded). The additional feature in (c) is ascribed to an impurity of unknown nature.

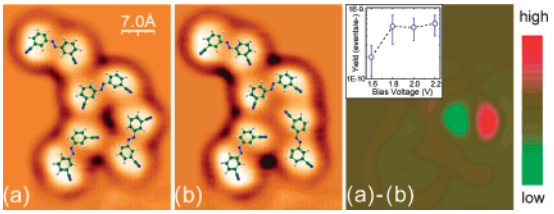

Figure 4. (a,b) Two successive STM images of a DMC island before and after a 4 s pulse of 1.7 V and 6 nA was applied. (a − b) shows the difference between the two images. The red to green motion reveals a change in one of the lobes of a molecule from 3,5′ to 3,3′. (a,b) Laplace filtered[28] to emphasize the molecular conformation. (3.5 × 4.6 nm^2; I_t = 3.2 nA; V_s = 0.5 V). The inset shows the resulting quantum yield after analyzing 123 manipulation events of DMC islands (rotating, diffusion, and phenyl rotation) for different bias voltages.

ably through δ^- (CN)− δ^+ (HC) H-bridge bonds, increasing their stability against the effect of tunnel electron. Figure 4 shows the result of applying a 1.7 V pulse on a small cluster of molecules. In this case, only one single molecule changes from a 3,5′ to a 3,3′ conformer. In most cases, the result of electron injection into one molecule is the collective motion of several molecules in a cluster, indicating that their interaction is strong enough to couple their motion. This coupling between molecules also hinders the manipulation process. The quantum yield for inducing molecular motion (diffusion, rotation, or ring-flip) in DMC islands is roughly estimated as 5×10^{-10} (see inset in Figure 4), which is 10 times smaller than that for the case of single molecules. This value, however, is an average of various molecular islands, and for each case, it will depend on the number of H-bridge bonds fixing the molecule in the cluster. The threshold for changes in the structure of DMC in islands is about 1.7 eV (Figure 4), similar to the one found in single molecules (Figure 2).

C. Tunneling Spectroscopy. The threshold bias of ∼1.7 V found in our experiment is a fingerprint of the molecular excitation leading to both molecular motion and phenyl ring rotation. Electron induced processes may involve either the electronic excitation of transient molecular states[15,16,18,30] or the excitation of molecular vibrations through inelastic scattering.[31−33] Both types of excitation can also activate conformational

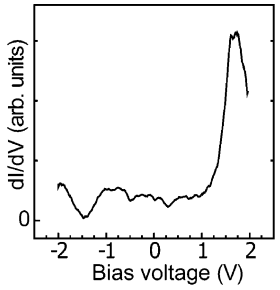

Figure 5. Tunneling spectrum of a DMC molecule. The resonance at 1.7 eV is associated with the first unoccupied molecular π^* orbital (LUMO) by which the conformational change seems to be initiated.

changes in molecules.[9,24,34] To find out which of the two mechanisms applies, here, we compare the threshold for switching with the energy alignment of molecular states derived from the DMC on Au(111), measured using scanning tunneling spectroscopy (STS). In STS, the tunneling junction's differential conductivity (dI/dV) is related to the molecular or surface density of electronic states. dI/dV curves are obtained by means of a lock-in during a current−voltage characteristic. The spectrum in Figure 5 is acquired on top of a DMC molecule forming part of a molecular cluster in order to hinder the fast motion of the molecule during the measurement. The spectrum shows a clear enhancement of the differential conductance at 1.7 V. This is interpreted as being due to electron tunneling through molecular resonances derived from the lowest unoccupied molecular orbital (LUMO) of the DMC molecule. The close correspondence of the energy alignment of this molecular resonance with the ∼1.7 V threshold for switching strongly supports that the switching dynamics is activated by electron scattering with this unoccupied molecular state.

D. Intramolecular Dynamics. The energy position of the resonance found in the tunneling spectrum can be interpreted on the basis of first principle calculations by Füchsel et al.[24] For a free trans isomer, the authors find an electron affinity (EA) of about 1.9 eV. The vertical excitation energy to an anion state of DMC adsorbed on Au(111) can be estimated from $\Delta E = \phi - \mathrm{EA} - e^2/4Z$, where ϕ = 5.1 eV is the Au(111) work function and the last term accounts for the stabilization of the excitation energy due to image charge screening at a molecule−surface distance Z. The peak alignment of about 1.7 V in Figure 5 requires an image charge stabilization of about 1.5 eV, which is fully consistent with the present molecule−surface distances.

In gas phase, the electronic population of affinity levels, that is, electron attachment, is an efficient method to induce chemical reactions.[35] For adsorbates on metal surfaces, electron tunneling is generally a fast process, much faster than nuclear motion. Therefore, electronic excitations are not an efficient way to induce molecular transformations. However, the topology of anionic potential energy surfaces (PES) can help to accelerate the nuclei along specific reaction coordinates, which might eventually lead to a transformation after quenching to the ground state.[24] It is thus important to rationalize our results in terms of the intramolecular dynamics driving the ring rotation.

For DMC on Au(111), the two ground state conformations (3,3′ and 3,5′) are supposedly connected through a potential energy barrier essentially composed of the free-molecule β-rotation barrier (see below) plus the potential energy due to the interaction of the phenyl ring with the Au(111) surface. From our experiments, we conclude that electron tunneling through the anionic resonance is able to rotate one of the DMC phenyl rings along the β angle. This rotation necessarily implies the existence of a nonplanar intermediate configuration. The detailed

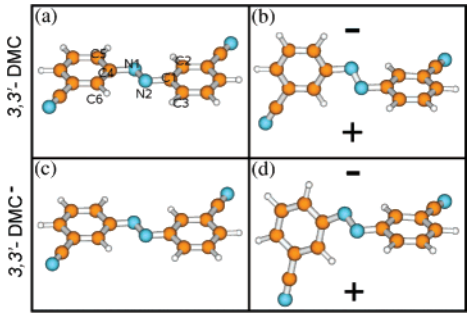

Figure 6. Optimized structures of 3,3′-DMC without (a) and with field (b) and of 3,3′-DMC$^-$ (anion) without (c) and with field (d). In (b,d), the field is oriented perpendicular to the right N−Ph−CN ring, assuming that it is kept parallel to the substrate's surface plane. The field direction is from the "surface" (+) to the "tip" (−). In (a), some atoms are labeled. Note that in the field-on case, there are in general four different β angles, those connecting N1−N2 with C1 and C2, C1 and C3, C4 and C5, or with C4 and C6. In this work, we refer always to the N1−N2−C1−C2 dihedral angle.

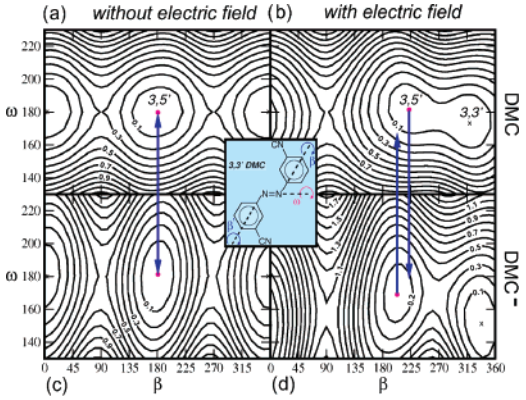

Figure 7. Contour plots of potential energy surfaces $V(\beta,\omega)$ of DMC without (a) and with field (b), DMC$^-$ (anion) without (c) and with field (d). All contours are spaced by 0.1 eV, starting from the absolute minima. Values are attached to some of the contours. The coordinates β and ω are indicated as an inset again for clarity. The arrows indicate the process of sudden, vertical electron attachment/detachment processes. In the field-free case, not much energy is gained or lost upon attachment [a → c] or detachment [c → a] because the 3,5′ minima for DMC and DMC$^-$ are at the same positions. In contrast in the field-on case, by sudden attachment [b → d] or detachment processes [d → b] energy can be gained to overcome the barrier for isomerization toward the 3,3′ minimum in (b). When further modes are included, the energy gain δE according to eq 1, is even bigger than suggested by the figure (see text).

structure of the transition state can only be described after knowledge of the intramolecular pathway followed during the excitation. This pathway is expected to be complex because of the interaction with the surface and to the electric field existing at the tunneling junction. On Au(111), DMC is presumably adsorbed with a planar configuration because the physical interaction with the metal is governed by the phenyl π states. It is then justified to present in the next section a model theoretical approach on a free planar molecule aiming at rationalizing how a fast electronic excitation can couple with internal motion out of its planar structure.

It is helpful to argue the time scale of the ring-rotation mechanism based on the experimental quantum yield Y_R. For the isolated molecule on the Au(111) surface, we estimate roughly $Y_R \sim 10^{-9}$. This low value is a consequence of the short excitation lifetime τ_e with respect to the time required to rotate the ring. From the line width of the LUMO resonance in the STS data of Figure 5 ($\Gamma \sim 450$ mV), we may approximate $\tau_e = \hbar/\Gamma \sim 1.5$ fs. It is then reasonable to expect that the complete internal dynamics leading to the ring rotation takes place in the electronic ground state, and it is eventually triggered by the fast electron scattering with the LUMO resonance.

E. Quantum Chemical Calculations. The scenario of a negative-ion resonance mediated reaction is supported by quantum chemical calculations. For the calculations, the hybrid B3LYP functional of density functional theory and a 6-31G* basis set were employed as implemented in the Gaussian03 program suite.[36]

Using this method, we computed for a free molecule, one-dimensional potential energy curves $V(\beta)$ along β, which is the dihedral angle defined by the central NN bond and two neighboring C atoms of the rotating phenyl rings (the N1−N2−C1−C2 dihedral according to Figure 6a). In addition, we computed two-dimensional (2D) potential energy surfaces $V(\beta,\omega)$ where also the CNNC dihedral ω (connecting C4−N1−N2−C1 atoms in Figure 6) was included. These potential curves and surfaces were calculated for DMC and DMC$^-$, with and without an external electric field.

In the two-dimensional model, β was varied in the interval [0°,360°] and ω in the interval [130°,230°]. All other internal coordinates were fixed at values which were obtained from a full geometry optimization of the 3,3′ structure of neutral DMC. Precisely the same, restricted geometries were then used for three other potential surfaces, namely, those of DMC$^-$ anion in the absence of a field and of DMC and DMC$^-$ in an external, homogeneous electric field. The field was perpendicular to one-half of the molecule, that is, the right N−Ph−CN unit in Figure 6, which was forced to stay flat in a plane (assumed parallel to the substrate's surface), while the other half was free to move along ω and β modes. The field strength was $F = 0.4$ V/Å and was directed from the surface (+) to the tip (−). The field orientation is consistent with experiment while its strength is probably somewhat too large.

In Figure 7, we show the restricted, two-dimensional potential energy surfaces $V(\beta,\omega)$ for all four situations [(a) DMC without field, (b) DMC with field, (c) DMC$^-$ without field, (d) DMC$^-$ with field]. For DMC without field (a), one finds minima at $\beta = 0°$, $\omega = 180°$ and $\beta = 180°$, $\omega = 180°$, corresponding to 3,3′ and 3,5′ conformations, respectively. The former is slightly more stable than the latter, by about 0.01 eV because of the more favorable antiparallel alignment of the dipole moments of the CN groups. A full geometry optimization (rather than a restricted one) gives the same minima, both what concerns energetics and geometry. The fully optimized structures of the 3,3′ form is shown in Figure 6a.

The 3,3′ and 3,5′ conformers are separated by a barrier of about 0.30 eV at $\beta = 90°$, $\omega = 180°$. For symmetry reasons, an equivalent barrier is found at $\beta = 270°$. We note that from a $V(\beta)$ curve (not shown) with fully relaxed, other internal coordinates, a barrier of 0.27 eV is found, demonstrating that the restricted 2D model works well.

When attaching an electron to free DMC (Figure 7c), the major effect is that the barrier increases to about 0.61 eV, with $\beta = 0°$ and $\beta = 180°$ still being minima. The same minima are found by full geometry optimization of DMC$^-$, as shown in Figure 6c. The increased barrier in the anion state is a result of the fact that the LUMO of the DMC molecule is bonding between the central N atom(s) and the nearby C atom(s) C1 or C4; see the figure of ref 24. Attaching an electron to this orbital will hinder rotation. In the one-dimensional (1D), fully relaxed model, the barrier for DMC$^-$ is 0.56 eV and thus similar.

The larger barrier in the anion state is not, per se, counterproductive for the 3,3′ ↔ 3,5′ isomerization if the reaction

proceeds predominantly in the neutral state after attachment and rapid detachment of the excess electron, as it is presumably occurring for DMC on a metallic surface. However, since the topologies of the DMC and DMC^- surfaces in Figure 7a,c are the same, no torque along the β coordinate is created by the attachment/detachment process, and the molecule would remain ideally flat and nonrotating. This conclusion is also confirmed by the fully optimized structures for (field-free) DMC and DMC^-, which are shown in Figure 6a,c. Upon electron attachment, the most dramatic changes occur in the central C−N−N−C unit of the molecule. Because of the N−N antibonding and N−C bonding character of the LUMO of neutral DMC, the N−N bond of DMC^- is elongated by about 0.07 Å relative to DMC, while the N−C bond length shrinks by about 0.05 Å. None of these modes will rotate one of the phenyl rings relative to the other, if excited.

A torque along β (and ω), however, might be exerted because of the electric field effects and the presence of the surface. To demonstrate the effect of the former, we show in Figure 7b,d the contour plots of the restricted 2D potential energy surfaces $V(\beta,\omega)$ for neutral DMC and anionic DMC^-, when a field is applied.

Let us consider neutral DMC first. From Figure 7b, we find that the 3,3′ minimum shifts by about $-40°$ along β and $-10°$ along ω, to about $\beta = 320°$, $\omega = 170°$. Similarly, the 3,5′ minimum shifts by about $+40°$ along β and along ω, to about $\beta = 220°$, $\omega = 175°$. The fully optimized structure (with one N−Ph−CN kept flat and parallel to the substrate surface, interatomic distances optimized) is shown in Figure 6b. It is found that DMC adopts a more three-dimensional shape in order to minimize its energy in the external field by orienting the CN group of the mobile phenyl ring toward the surface. This maximizes the attractive Coulomb interaction between the negatively charged N atom with the "positive surface" underneath.

From Figure 7b, we also note that the two transition states at $\beta \approx 90°$ and $\beta \approx 270°$ become inequivalent, when the field is on. One of the barriers, at $\beta \approx 90°$, is about 0.7 eV and thus higher than in the field-free case (0.3 eV according to Figure 7a), while the other barrier at $\beta \approx 270°$ decreases somewhat, to less than 0.1 eV. The inequivalent barriers are due to the cyano group of the rotating phenyl ring pointing either toward the "positive surface" (for $\beta = 270°$) or toward the "negative tip" (for $\beta = 90°$), leading to enhanced Coulomb attraction (for $\beta = 270°$) or repulsion (for $\beta = 90°$). In the 1D $V(\beta)$ model, with partial relaxation of other internal molecular modes, the lower barrier is about 0.15 eV, with the higher barrier at 0.8 eV. In the experiments, the barriers will increase because of the physisorption of DMC on the surface. Hence, a realistic estimation for the barriers would be in the order of 0.4 eV to more than 1 eV, depending on the direction of the rotation.

When attaching an electron the situation changes. From comparison of Figure 7b,d but also from the optimized structures in Figure 6b,d, we note that in the anion the minimum-energy geometries are shifted relative to the neutral molecule, particularly by the angles β and ω. This is different from the field-free case. Since the minima in Figure 7b,d are now at different positions, electron attachment will induce a (coupled) motion along the β and ω coordinates, toward the shifted minima. In the anion state, the ω shift is larger than in the neutral state, that is, the molecule is more three-dimensional as an anion state if the field is on. Detachment of the electron from DMC^- (Figure 7d) will bring the system back to the neutral DMC surface (Figure 7b), where additional kinetic energy can be gained by motion toward the minima of the neutral surface.

An upper bound of the energy gain by attachment and subsequent detachment can be estimated as follows. We first optimize the geometry of DMC and that of DMC^-, giving structures denoted here by (a set of) coordinates Q_{DMC} and Q_{DMC^-}, respectively, with corresponding energies $E_{DMC}(Q_{DMC})$ and $E_{DMC^-}(Q_{DMC^-})$. We then calculate the energies of the anion, DMC^-, at the neutral DMC geometry Q_{DMC}, giving $E_{DMC^-}(Q_{DMC})$, as well as $E_{DMC}(Q_{DMC^-})$ which is the energy of neutral DMC at the DMC^- optimized geometry Q_{DMC^-}. The maximal energy to be gained is the sum of two contributions, namely, the energy difference between an anion, suddenly created by electron attachment to neutral DMC and the energy minimum of DMC^-, and a corresponding term for the subsequent detachment process:

$$\delta E = [E_{DMC^-}(Q_{DMC}) - E_{DMC^-}(Q_{DMC^-})] + [E_{DMC}(Q_{DMC^-}) - E_{DMC}(Q_{DMC})] \quad (1)$$

The maximal energy gain δE according to eq 1 is about 0.45 eV for the field-free and about 2.1 eV for the field-on case, respectively. In particular, this last value shows that a substantial amount of energy may be gained during an attachment/detachment process to overcome a typical β-rotation barrier. This is expected to remain true even if additional distortions due to the surface were accounted for and even if one acknowledges that the field used here is probably somewhat too high.

It must be noted, however, that only detailed multidimensional dynamics calculations as well as the explicit inclusion of the surface can prove as to whether the energy is channelled into the right directions and thus as to whether the suggested mechanism is operative.

III. Conclusions

DMC azobenzene derivatives are found in two stable trans conformations (3,3′ and 3,5′) on the Au(111) surface, which are connected through the rotation of a phenyl ring. We have demonstrated that the switching between these rotamers can be induced by electrons tunneling through the LUMO resonance, located at 1.7 eV above the Fermi level. This process can be explained if the fast electron scattering with a negative ion resonance induces a temporary change in geometry. The coupling to rotational motion is possibly linked to electric field effects or to nonplanar molecular geometry (not considered here). The internal rotation probably occurs in the neutral state, which is compatible with the short time-scale of molecular electronic excitations on metallic substrates. Hence, a phenyl ring rotation around the β axis becomes possible and leads to a change between the 3,3′ and 3,5′ structures at the surface. Our results can be extended to understand which is the role of the adsorption configuration in molecular handling at surfaces using tunneling electrons. On Au(111), the molecular structure is presumably planar. Therefore, we expect that the electron-induced three-dimensional conformational motion can be enhanced if the planar molecular structure is strongly distorted by the functionalization with different end groups or by the formation of a stronger chemical bond to a more reactive surface.

Acknowledgment. We thank R. Rurali for fruitful discussion and M. Alemani and J. Henzl for sharing their manuscripts before publication. We acknowledge technical support by C.

Roth and M. Alemani. This research was supported by the Deutsche Forschungsgemeinschaft, SFB 658. I.F.T. acknowledges financial support from the Generalitat de Catalunya.

References and Notes

(1) Feringa, B. L., Ed. *Molecular switches*; Wiley−VCH: Weinheim, Germany, 2001; ISBN 3527299653.

(2) Wachtveitl, J.; Sporlein, S.; Satzger, H.; Fonrobert, B.; Renner, C.; Behrendt, R.; Oesterhelt, D.; Moroder, L.; Zinth, W. *Biophys. J.* **2004**, *86*, 2350.

(3) Sekkat, Z.; Knoll, W. *Photoreactive organic thin films;* Elsevier Science: San Diego, CA, 2002; ISBN 0126354901.

(4) Hugel, T.; Holland, N. B.; Cattani, A.; Moroder, L.; Seitz, M.; Gaub, H. E. *Science* **2002**, *296*, 1103.

(5) Zhang, C.; Du, M.-H.; Cheng, H.-P.; Zhang, X.-G.; Roitberg, A. E.; Krause, J. L. *Phys. Rev. Lett.* **2004**, *92*, 158301.

(6) Elsässer, T., Fujimoto, J., Wiersma, D., Zinth, W., Eds. *Ultrafast Phenomena XI;* Springer: Berlin, Germany, 1998; ISBN 3540654305.

(7) Nägele, T.; Hoche, R.; Zinth, W.; Wachtveitl, J. *Chem. Phys. Lett.* **1997**, *272*, 489.

(8) Dulic, D.; van der Molen, S. J.; Kudernac, T.; Jonkman, H. T.; de Jong, J. J. D.; Bowden, T. N.; van Esch, J.; Feringa, B. L.; van Wees, B. J. *Phys. Rev. Lett.* **2003**, *91*, 207402.

(9) Gaudioso, J.; Lauhon, L. J.; Ho, W. *Phys. Rev. Lett.* **2000**, *85*, 1918.

(10) Henzl, J.; Mehlhorn, M.; Gawronski, H.; Rieder, K.-H.; Morgenstern, K. *Angew. Chem., Int. Ed.* **2006**, *45*, 603.

(11) Choi, B.-Y.; Kahng, S.-J.; Kim, S.; Kim, H.; Kim, H. W.; Song, Y. J.; Ihm, J.; Kuk, Y. *Phys. Rev. Lett.* **2006**, *96*, 156106.

(12) Henzl, J.; Bredow, T.; Morgenstern, K. *Chem. Phys. Lett.* **2007**, *435*, 278.

(13) Qiu, X. H.; Nazin, G. V.; Ho, W. *Phys. Rev. Lett.* **2004**, *93*, 196806.

(14) Alemani, M.; Peters, M.; Hecht, S.; Rieder, K.-H.; Moresco, F.; Grill, L. *J. Am. Chem. Soc.* **2006**, *128*, 14446.

(15) Iancu, V.; Hla, S.-W. *PNAS* **2006**, *103*, 13718.

(16) Stokbro, K.; Thirstrup, C.; Sakurai, M.; Quaade, U.; Hu, B. Y. K.; Perez-Murano, F.; Grey, F. *Phys. Rev. Lett.* **1998**, *80*, 2618.

(17) Lastapis, M.; Martin, M.; Riedel, D.; Hellner, L.; Comtet, G.; Dujardin, G. *Science* **2005**, *308*, 1000.

(18) Sloan, P. A.; Palmer, R. E. *Nature* **2005**, *434*, 367.

(19) Priewisch, B.; Rück-Braun, K., unpublished results.

(20) Priewisch, B.; Rück-Braun, K. *J. Org. Chem.* **2005**, *70*, 2350.

(21) Spagnolo, P.; Testafer, L.; Tiecco, M. *J. Chem. Soc. B* **1971**, *1971*, 2006.

(22) Tsuji, T.; Takashima, H.; Takeuchi, H.; Egawa, T.; Konaka, S. *J. Mol. Struct.* **2000**, *554*, 203.

(23) Tsuji, T.; Takashima, H.; Takeuchi, H.; Egawa, T.; Konaka, S. *J. Phys. Chem. A* **2001**, *105*, 9347.

(24) Füchsel, G.; Klamroth, T.; Dokić, J.; Saalfrank, P. *J. Phys. Chem. B* **2006**, *110*, 16337.

(25) Weigelt, S.; Busse, C.; Petersen, L.; Rauls, E.; Hammer, B.; Gothelf, K. V.; Besenbacher, F.; Linderoth, T. R. *Nat. Mater.* **2006**, *5*, 112.

(26) Barth, J. V.; Brune, H.; Ertl, G.; Behm, R. J. *Phys. Rev. B* **1990**, *42*, 9307.

(27) The STM hardly can identify the cis or trans shape of the connecting backbone. Instead, we have compared these results with a similar molecular specie functionalized on para sites (diparacyano azobenzene (DPC)), because here the rotation around β leaves the molecular appearance unchanged. In this case only, features associated to trans isomers can be observed on the Au(111) surface. The absence of *cis*-DPC on the Au(111) indicates that a planar cis conformation is not a stable configuration, which presumably also applies to DMC.

(28) Horcas, I.; Fernández, R.; Gómez-Rodríguez, J.; Colchero, J.; Gómez-Herrero, J.; Baró, A. *Rev. Sci. Inst.* **2007**, *78*, 013705.

(29) When DMC is dosed on the Au(111) surface at room temperature highly ordered domains are formed, stabilized by H-bridge bonds. In this case, no successful conformational change could be observed.

(30) Müller, B.; Nedelmann, L.; Fischer, B.; Brune, H.; Barth, J. V.; Kern, K. *Phys. Rev. Lett.* **1998**, *80*, 2642.

(31) Ho, W. *J. Chem. Phys.* **2002**, *117*, 11033.

(32) Komeda, T.; Kim, Y.; Kawai, M.; Persson, B. N. J.; Ueba, H. *Science* **2002**, *295*, 2055.

(33) Pascual, J. I.; Lorente, N.; Song, Z.; Conrad, H.; Rust, H.-P. *Nature* **2003**, *423*, 525.

(34) Tanaka, S.; Itoh, S.; Kurita, N. *Chem. Phys. Lett.* **2002**, *362*, 467.

(35) Ingolfsson, O.; Weik, F.; Illenberger, E. *Int. J. Mass Spectrom.* **1996**, *155*, 1.

(36) Frisch, M. J.; Trucks, G. W.; Schlegel, H. B.; Scuseria, G. E.; Robb, M. A.; Cheeseman, J. R.; Montgomery, J. A., Jr.; Vreven, T.; Kudin, K. N.; Burant, J. C.; Millam, J. M.; Iyengar, S. S.; Tomasi, J.; Barone, V.; Mennucci, B.; Cossi, M.; Scalmani, G.; Rega, N.; Petersson, G. A.; Nakatsuji, H.; Hada, M.; Ehara, M.; Toyota, K.; Fukuda, R.; Hasegawa, J.; Ishida, M.; Nakajima, T.; Honda, Y.; Kitao, O.; Nakai, H.; Klene, M.; Li, X.; Knox, J. E.; Hratchian, H. P.; Cross, J. B.; Bakken, V.; Adamo, C.; Jaramillo, J.; Gomperts, R.; Stratmann, R. E.; Yazyev, O.; Austin, A. J.; Cammi, R.; Pomelli, C.; Ochterski, J. W.; Ayala, P. Y.; Morokuma, K.; Voth, G. A.; Salvador, P.; Dannenberg, J. J.; Zakrzewski, V. G.; Dapprich, S.; Daniels, A. D.; Strain, M. C.; Farkas, O.; Malick, D. K.; Rabuck, A. D.; Raghavachari, K.; Foresman, J. B.; Ortiz, J. V.; Cui, Q.; Baboul, A. G.; Clifford, S.; Cioslowski, J.; Stefanov, B. B.; Liu, G.; Liashenko, A.; Piskorz, P.; Komaromi, I.; Martin, R. L.; Fox, D. J.; Keith, T.; Al-Laham, M. A.; Peng, C. Y.; Nanayakkara, A.; Challacombe, M.; Gill, P. M. W.; Johnson, B.; Chen, W.; Wong, M. W.; Gonzalez, C.; Pople, J. A. Gaussian, Inc.: Wallingford, CT, 2004.